Electronic Supplementary Material (ESI) for ChemComm.

Supplementary Materials

Bifunctional covalent bromine: an advanced redox mediator for rechargeable lithium-oxygen batteries

Chu-Yue Li [a], Min-Sheng Wu [a], Wei-Rong Chen [a], Yuan-Jia Rong [a], Qian-Yan Wang [a], Xiao-Ping Zhang [a]*

a School of Electrical Engineering, Southwest Jiaotong University, Chengdu, 610031, China

**E-mail: zxp@swjtu.edu.cn*

Experimental Section[1-3]

MWCNT cathode

MWCNT (XFNANO, 8-15nm), single layer graphene and polyvinylidene fluoride (PVDF) were mixed with weight ratio of 8:1:1 in N- methyl- 2-pyrrolidone (NMP). The mixture was ultrasonicated for 30 minutes followed by magnetic stirring for 24 hours. And then, the slurry was casted onto the round- shape carbon paper with a diameter of 11 mm and a thickness of ~0.2 mm and vacuum dried at 80 ℃ for 24 hours. The loading weight of the cathode was ~0.1mg. The loading area was ~0.25 cm^2.

Li anode

The Li foil of thickness 0.2 mm was cut into 15.6 mm diameter discs.

Cu foil

A 0.2 mm thick Cu foil was cut into a disc of 11.0 mm in diameter.

Assembling Li-O_2 coin cell

Two-electrode system cells were assembled using CR2032-type coin cells with hole for O_2 channel in an Ar-filled glove box (O_2 and H_2O < 0.01 ppm). The lithium-oxygen batteries were assembled with MWCNT cathode, Waterman GF/A glass fiber separators and lithium metal anodes. The amount of 1.0 M lithium bis(trifluoromethane sulfonyl)imide/ Methyl

sulfoxide (LiTFSI/ DMSO) electrolyte in a coin cell is ~120 μL. 100 mM lithium bromide (LiBr，Adamas, 99.99%) or Trimethylbromosilane (C_3H_9BrSi, Sigma-Aldrich, 97%) is added as redox mediators. After assembly, the Li-O_2 batteries are transferred into a glass test chamber inflated with 1.0m bar of high-purity O_2 and rest for 3h.

Assembling Li | Li symmetric batteries and Li | Cu batteries

Symmetric Li | Li metal batteries are assembled using CR2032-type coin cells using the Li foil as working electrodes, Waterman GF/C as separator. The amount of 1.0 M lithium hexafluorophosphate/ ethylene carbonate / dimethyl carbonate ($LiPF_6$/EC/DMC) electrolyte in a coin cell was ~70 μL.

Li | Cu batteries were assembled using CR2025-type coin cells. The amount of 1.0 M Lithium hexafluorophosphate/ ethylene carbonate / dimethyl carbonate ($LiPF_6$/EC/DMC) electrolyte in a coin cell was ~70 μL. 100 mM lithium bromide (LiBr) or Trimethylbromosilane (C_3H_9BrSi) is added as redox mediators in both Li | Li symmetric batteries and Li | Cu batteries.

Electrochemical analysis

Galvanostatic discharging/ charging curve tests are using the LAND electrochemical testing system.

Cyclic voltammetry (CV) measurement is tested using Bio-logic VSP in the voltage range of 2.0-4.2 V at a scan rate of 0.1 mV/s.

Electrochemical Impedance Spectroscopy (EIS) is performed using Gamry Interface 5000 E with a voltage amplitude of 10 mV and a frequency range of 10^{6} to 10^{-1}.

Characterization

Lithium-oxygen batteries after cycling, are disassembled in the argon-filled glove box. Then, the anodes were washed in 1,2-Diethoxyethane (DME) for 30 min, and dried for 2 h.

The X-ray diffraction (XRD) measurements were used to characterize the LiOH on the pristine lithium anode on a Rigaku Ultima IV advanced diffractometer with Cu Kα radiation.

Field emission scanning electron microscopy (SEM) was used to observe the microstructure of the lithium anodes on Apreo 2C.

Fourier transform infrared spectroscopy (FTIR) was performed using a Bruker Scientific spectrometer (TENSOR II) from 4000 to 400 cm^{-1}.

The X-ray photoelectron spectroscopy (XPS) results were obtained on a Thermo Fisher ESCALAB Xi+ spectrometer with a monochromatic Al Kα X-ray source.

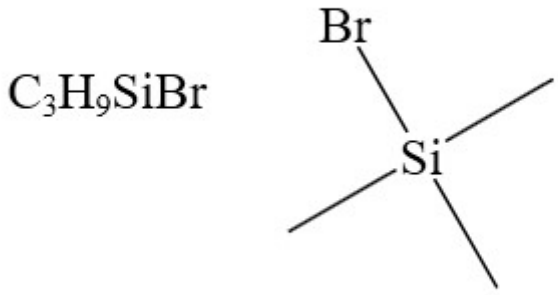

Fig S1. The structural formula of Trimethylbromosilane.

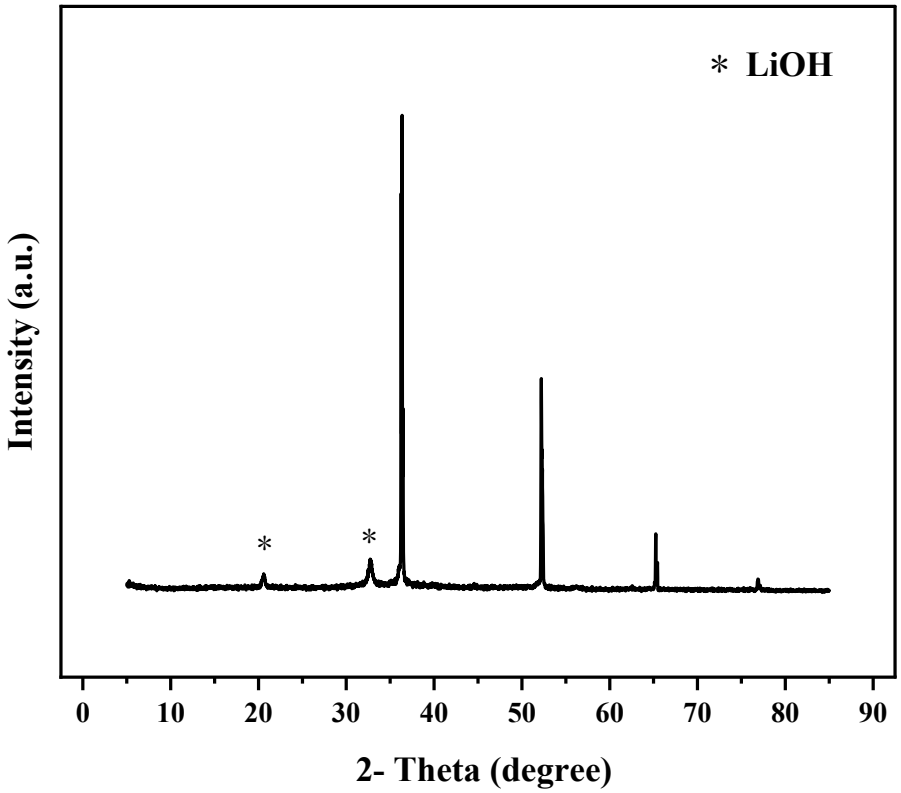

Fig. S2 XRD patterns of the pristine lithium anode.

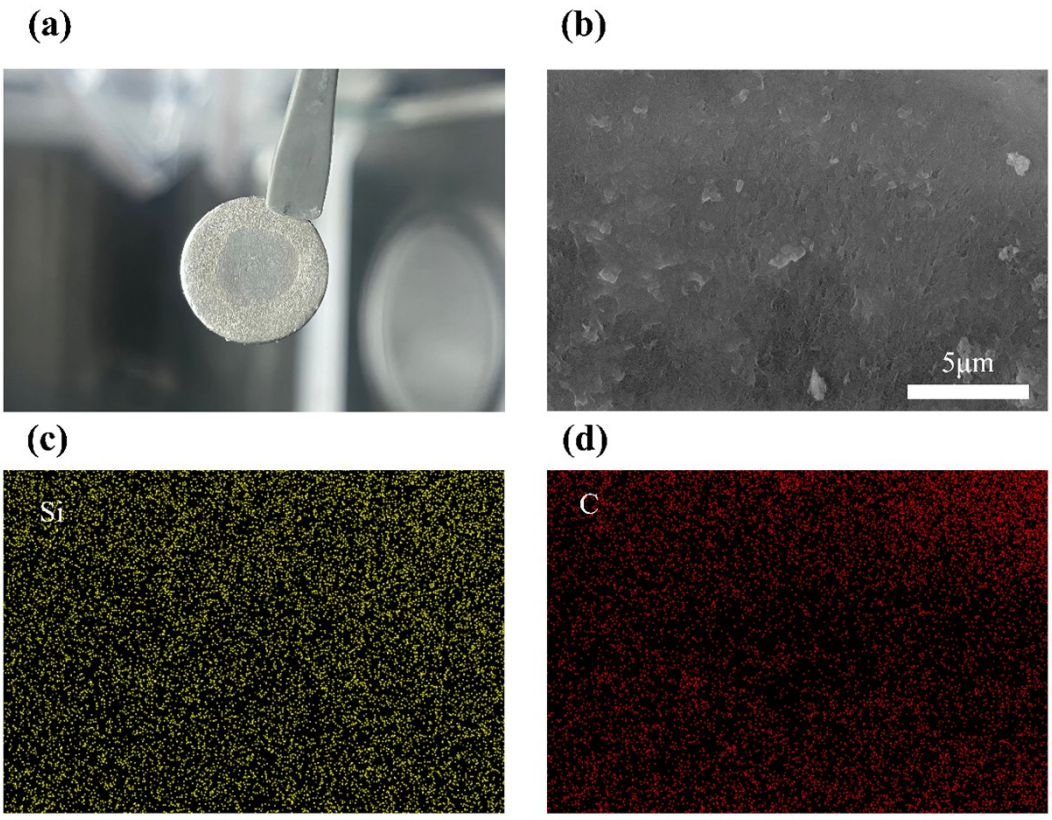

Fig. S3 (a) The digital photograph (b) SEM images of lithium metal dropping with 20μl C_3H_9SiBr. Energy dispersive spectroscopy (EDS) images of the top-view of the C_3H_9SiBr containing anode. (c) EDS spectra of Si (d) EDS spectra of C.

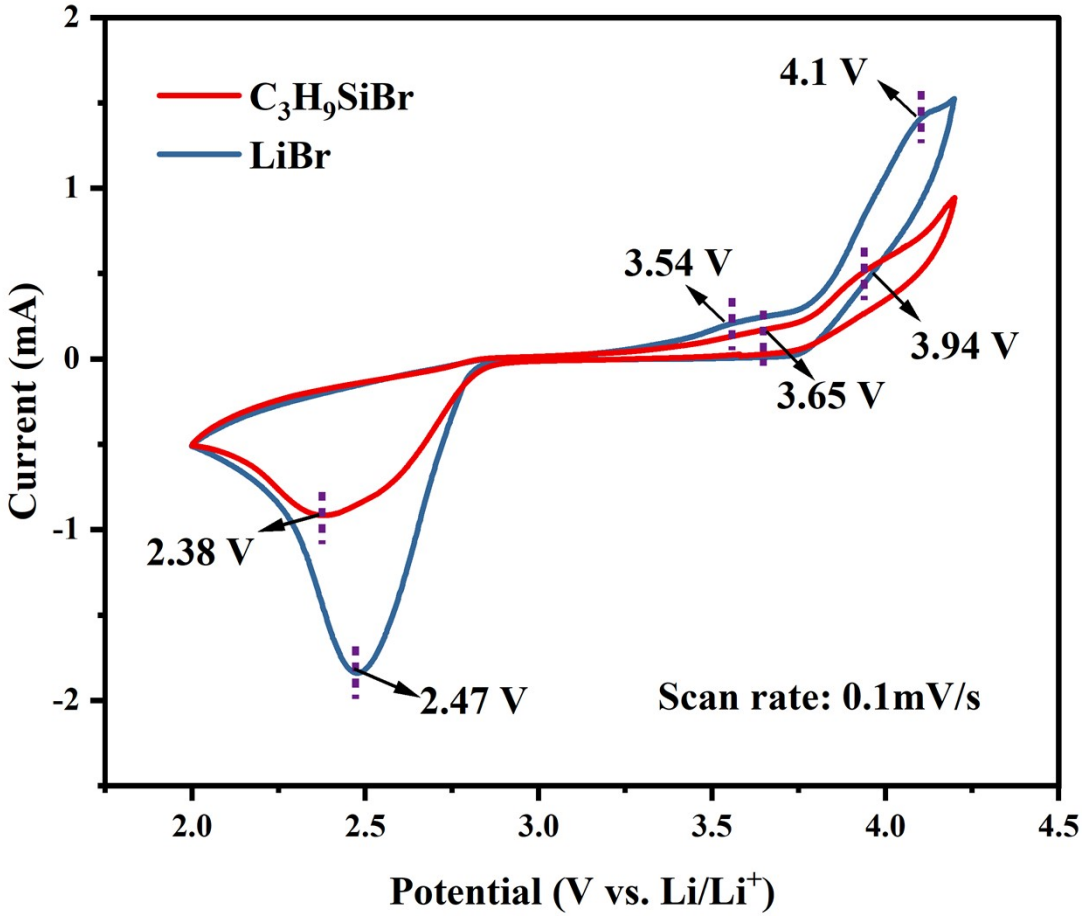

Fig. S4 Cyclic voltammogram (CV) curves of the lithium-oxygen batteries with C_3H_9SiBr or LiBr additive. The scan rate is 0.1 mV/s.

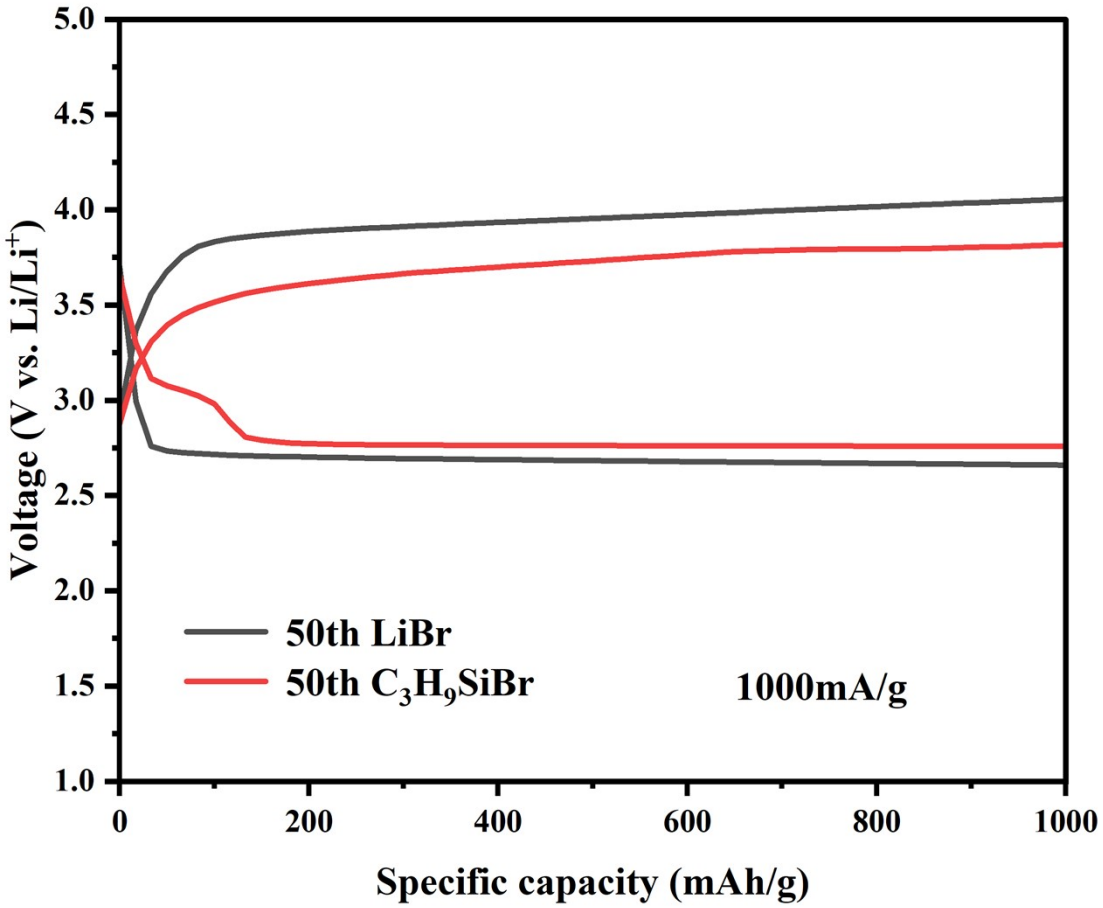

Fig. S5 Galvanostatic discharge/charge curves of the 50th cycle at 1000 mA/g.

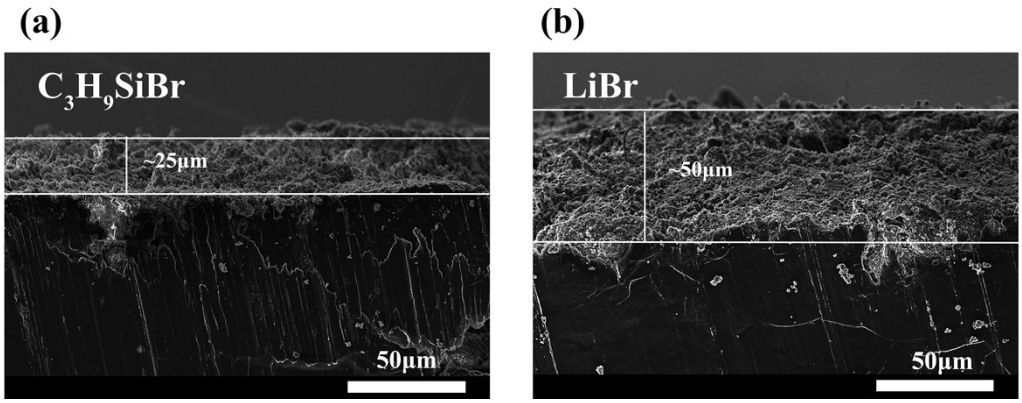

Fig. S6 Cross-section SEM images of lithium metal anodes after 30 cycles tested under a current density of 1000 mAh/g and a current at 1000 mA/ (a) C_3H_9SiBr-containing lithium metal anodes (b) LiBr-containing lithium metal anodes.

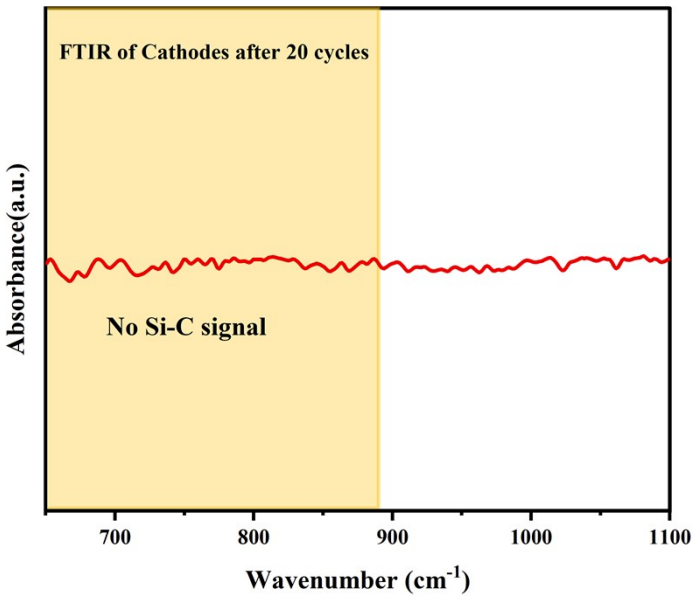

Fig. S7 FTIR spectra for the cathode in the C_3H_9SiBr-containing lithium-oxygen battery after 20 cycles.

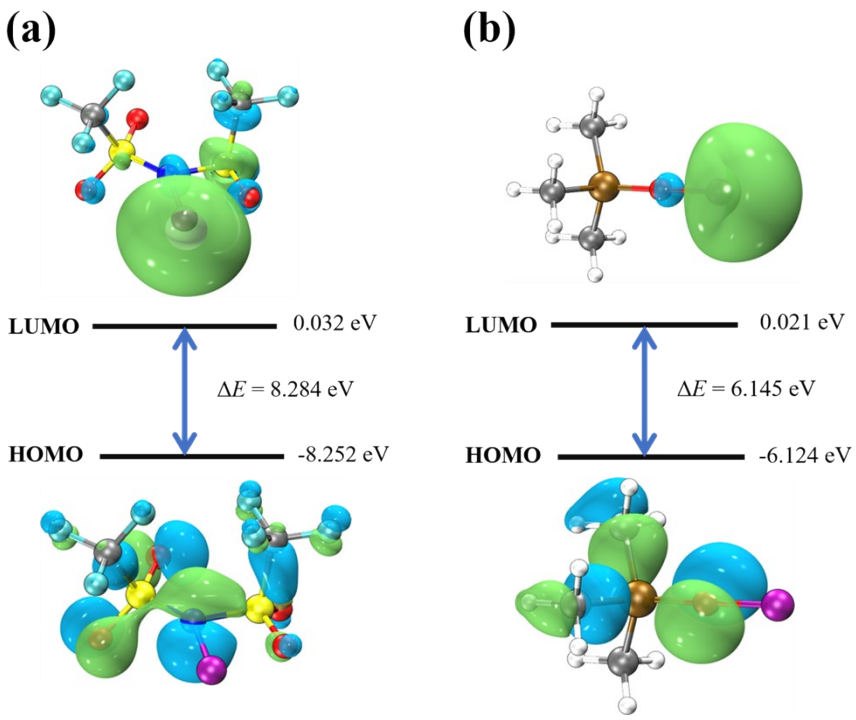

Fig. S8 LUMO and HOMO levels of (a)LiTFSI (b)C_3H_9SiOLi.

The theoretical calculations were performed via the Gaussian 16 suite of programs. The structures of two studied molecules were fully optimized at the B3LYP-D3BJ/6-31G(d) level of theory. The solvent (DMSO) effect was included in the calculations using the solvation model based on the density (SMD) model. The vibrational frequencies of the optimized structures were carried out at the same level. The structures were characterized as a local energy minimum on the potential energy surface by verifying that all the vibrational frequencies were real. The molecular orbital levels of studied compounds were investigated via theoretical calculations, including the highest occupied molecular orbital (HOMO) and the lowest unoccupied molecular orbital (LUMO). The Visual Molecular Dynamics (VMD) program was used to plot the color-filled iso-surface graphs to visualize the molecular orbitals.

FTIR and XPS are used to prove the existence of C_3H_9SiOLi on the surface of lithium metal anodes, which means C_3H_9SiOLi do not react with lithium metal during cycling. In order to evaluate the stability of SEI components quantitatively, calculations were conducted on the molecular orbital energies for the electron affinity and the chemical

reactivity of SEI components. As the LUMO level of C_3H_9SiOLi is lower than LiTFSI, which indicates that C_3H_9SiOLi is easier than LiTFSI to react with lithium metal during cycling. Now that we have proved C_3H_9SiOLi do not react with lithium metal during cycling, which means LiTFSI do not react with lithium metal either. These results can prove the stability of lithium-oxygen battery systems.

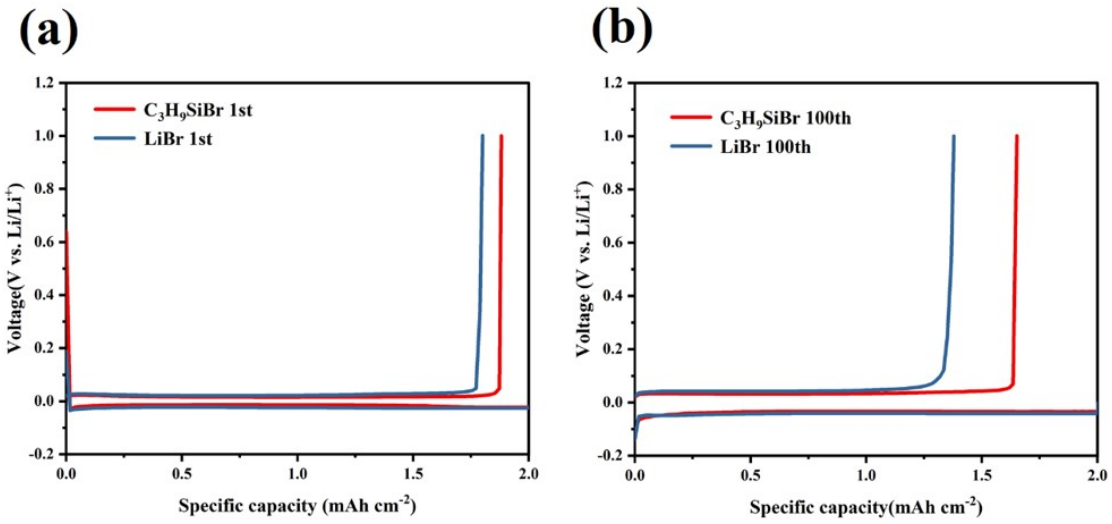

Fig. S9 Electrochemical performance of Li | Cu batteries. The electrodes are stripped/plated at a current density of 1 mA cm^{-2} with a fixed capacity of 2 mA h cm^{-2}. Galvanostatic discharge/charge profiles with 100 mM C_3H_9SiBr or LiBr additive at 1st cycle (a) 100th cycle (b).

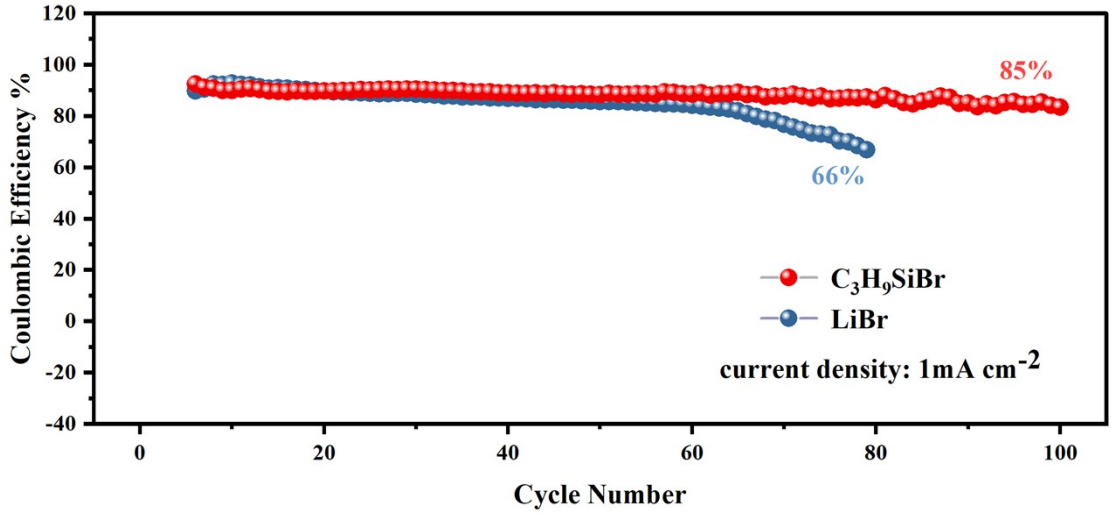

Fig. S10 The comparison of coulombic efficiency of C_3H_9SiBr or LiBr- containing Li | Cu cells

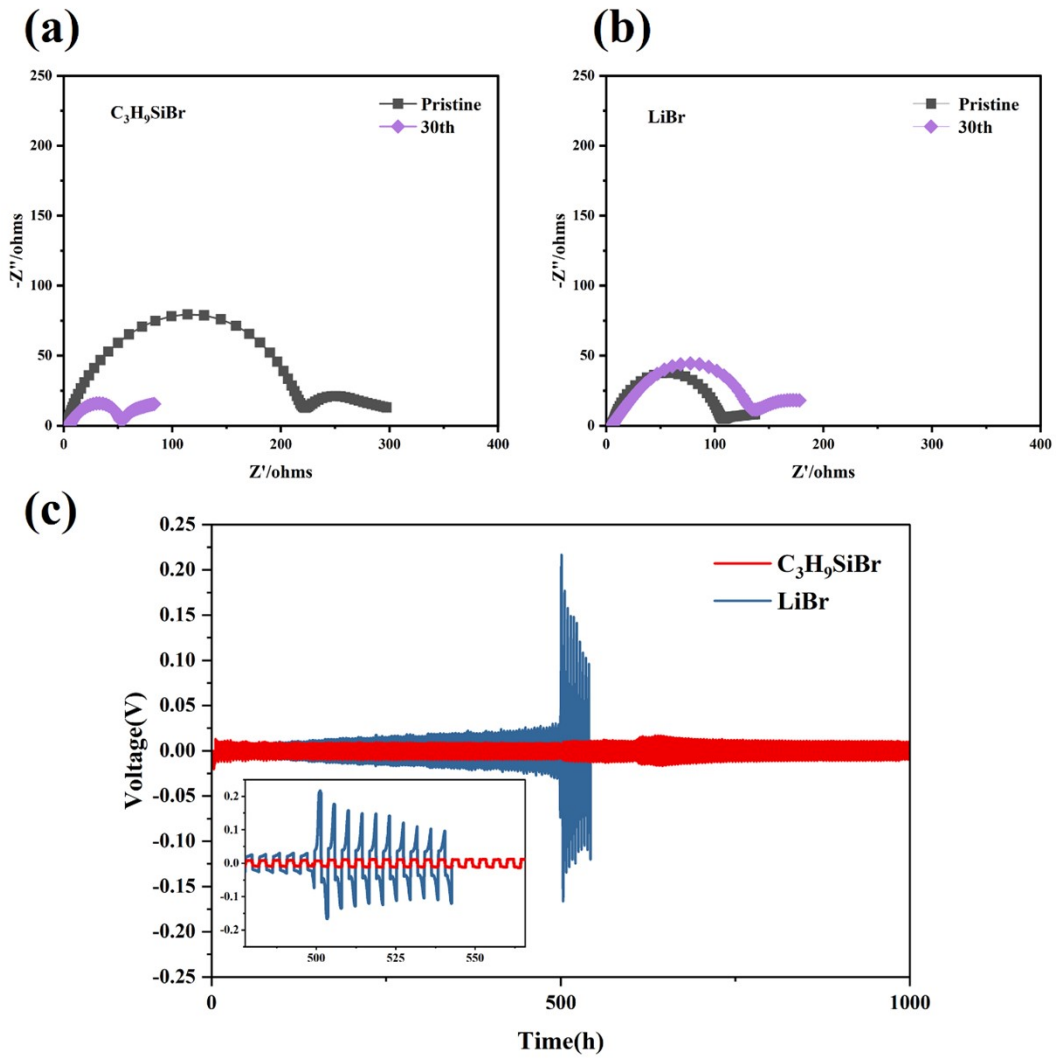

Fig. S11 EIS spectra for (a) C_3H_9SiBr (b) LiBr. (c) Electrochemical performance of Li | Li symmetric batteries.

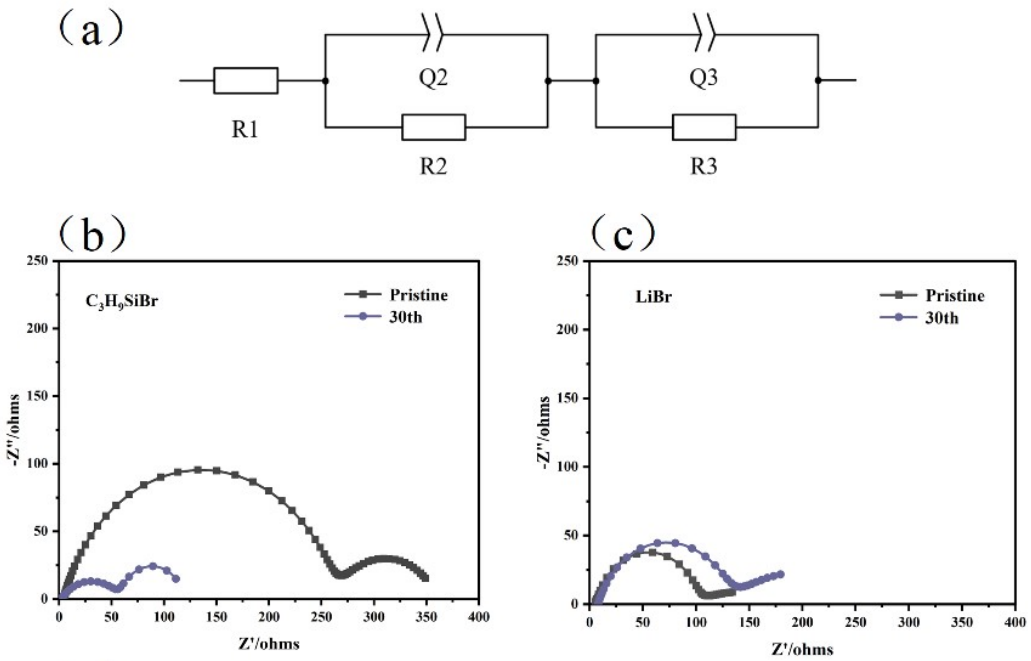

(d)

Working Electrode	cycle number	R_1/ohms	R_2/ohms	R_3/ohms
C_3H_9SiBr treated Li metal	pristine	4.419	96.01	260.3
	30th	2.148	61.42	56.83
LiBr treated Li metal	pristine	3.794	100.1	90.88
	30th	7.820	142.3	120.9

Fig. S12 EIS analysis corresponding to Fig. S11. EIS analysis with (a) equivalent circuit model (b) Nyquist plots of fitted results of C_3H_9SiBr-containing Li | Li symmetric batteries, (c) Nyquist plots of fitted results of LiBr-containing Li | Li symmetric batteries, (d) fitting parameters.

Two semicircles are exhibited in the C_3H_9SiBr-containing batteries. It is worth pointing out that the low-frequency semicircle appears to indicate the existence of a protective SEI layer on lithium metal electrodes. [4] Meanwhile, in the 30^{th} cycle, C_3H_9SiBr-containing batteries have a smaller charge-transfer resistance of 61.42 ohms than the LiBr-containing batteries (142.3 ohms), showing that the SEI film formed on the lithium metal electrodes is high ion-conductivity. From the fitting EIS analysis, it is further proved that the SEI layer has low interface impedance and high ion conductivity.

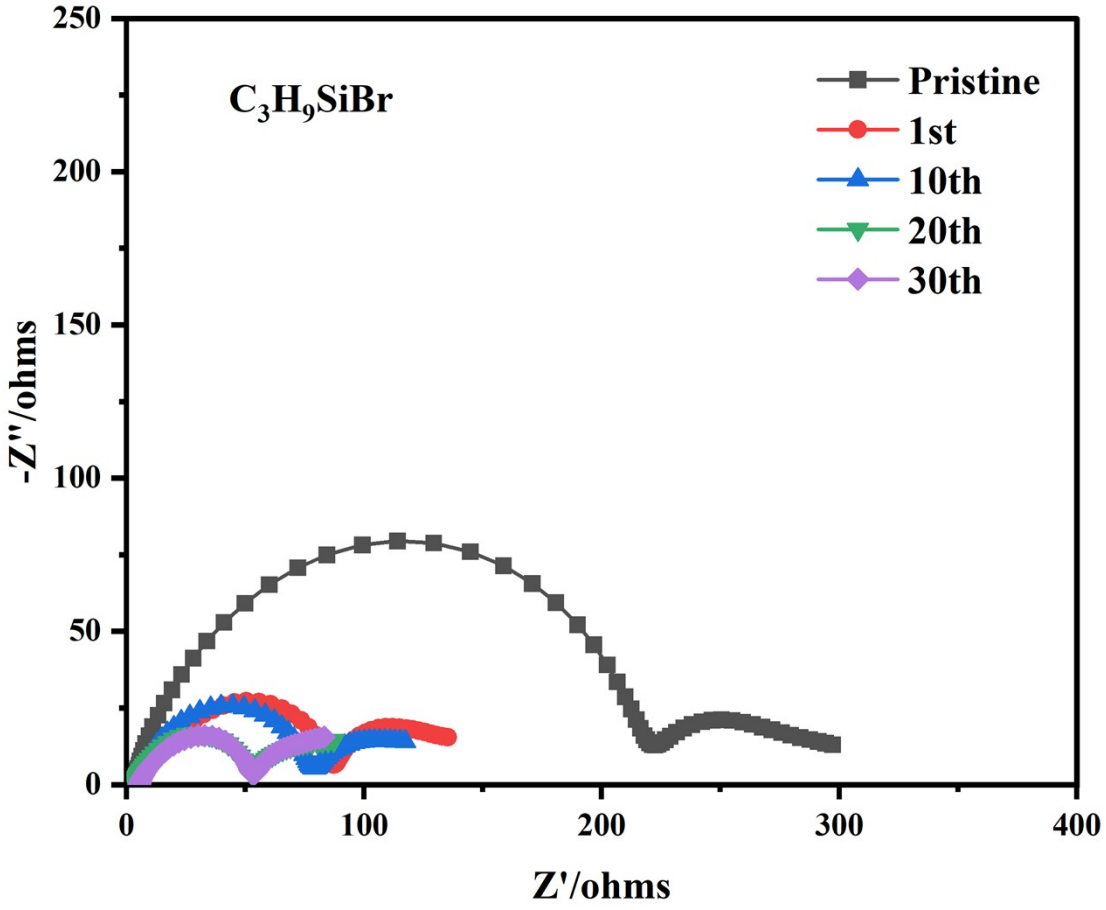

Fig. S13 The change of impedance for Li | Li symmetric batteries with C_3H_9SiBr.

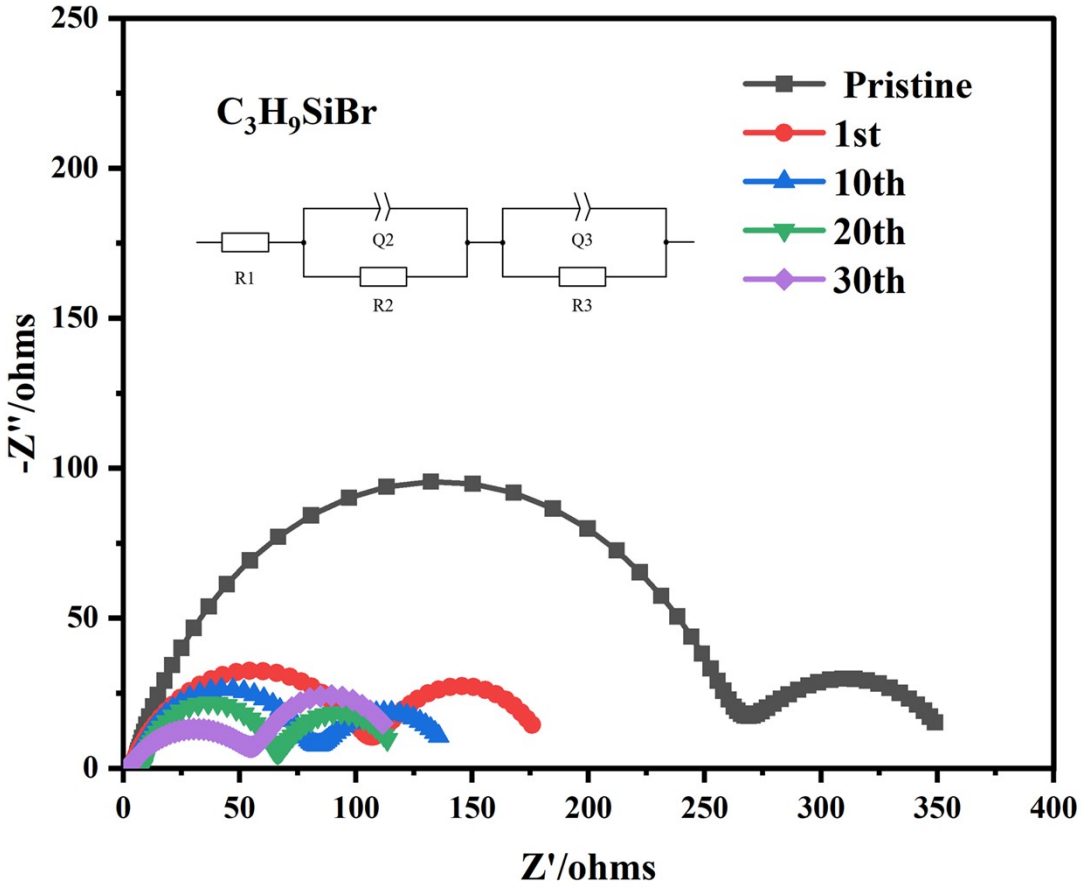

Fig. S14 EIS analysis corresponding to Fig. S13.

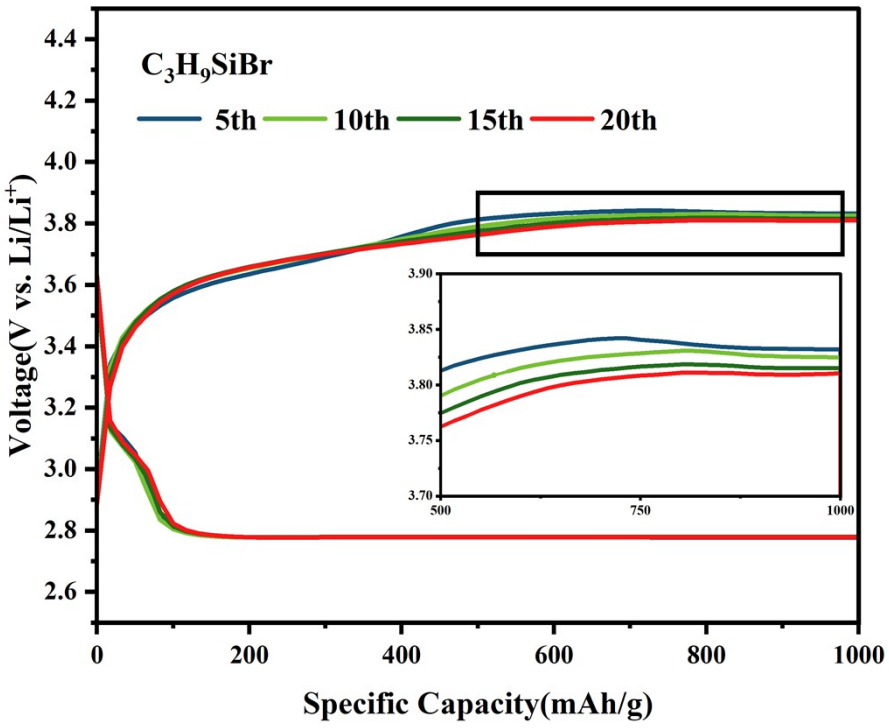

Fig. S15 Galvanostatic discharge/charge curves of the first 20 cycles at 1000 mA/g.

References

1. T. Zhang, K. Liao, P. He and H. Zhou, *Energy & Environmental Science*, 2016, **9**, 1024-1030.
2. Y. N. Li, F. L. Jiang, Z. Sun, O. Yamamoto, N. Imanishi and T. Zhang, *ACS Appl. Mater. Interfaces*, 2021, **13**, 16437-16444.
3. X. P. Zhang, Y. Y. Sun, Z. Sun, C. S. Yang and T. Zhang, *Nat Commun*, 2019, **10**, 3543.
4. T. S. Ong and H. Yang, *Electrochemical and Solid State Letters*, 2001, **4**, A89-A92.